

# Intrinsic AuPt-alloy particles decorated on TiO<sub>2</sub> nanotubes provide enhanced photocatalytic degradation

Beatriz Eugenia Sanabria-Arenas,<sup>[a,b]</sup> Anca Mazare,<sup>[b]</sup> Jeongeun Yoo,<sup>[b]</sup> Nhat Truong Nguyen,<sup>[b]</sup> Haidong Bian,<sup>[c]</sup> Maria Vittoria Diamanti,<sup>[a]</sup> Maria Pia Pedferri<sup>[a]</sup> and Patrik Schmuki<sup>\*[b,d]</sup>

<sup>a</sup> Politecnico di Milano, Department of Chemistry, Materials and Chemical Engineering “Giulio Natta”, Via Mancinelli 7, 20131 Milan, Italy

<sup>b</sup> Department of Materials Science, Institute for Surface Science and Corrosion WW4-LKO, Friedrich-Alexander University of Erlangen-Nuremberg, Martensstr 7, 91058 Erlangen, Germany

<sup>c</sup> Center of Super-Diamond and Advanced Films (COSDAF), City University of Hong Kong, Kowloon, Hong Kong, China

<sup>d</sup> Department of Chemistry, King Abdulaziz University, Jeddah, Saudi Arabia

\* Corresponding author: schmuki@ww.uni-erlangen.de

## Abstract

In this study we investigate the performance of noble metal co-catalysts on anodic TiO<sub>2</sub> nanotubes for the photocatalytic degradation of a model pollutant. We create the noble metal decoration (nanoparticles of Au, Pt and mixed AuPt) intrinsically and extrinsically. Intrinsic decoration is achieved using a noble metal containing titanium alloy for anodic tube growth. Extrinsic decoration is carried out by physical vapor deposition (PVD) of the same noble elements on pure titania tubes. We find AuPt intrinsic decoration to provide a significant enhancement for the photocatalytic decomposition of the model pollutant acid orange 7 (AO7) due to a synergistic effect in the formed AuPt alloy. The AuPt alloy provides a photocatalytic activity that is higher than comparable extrinsic decoration or single element (Pt or Au) intrinsic decoration.

**Keywords:** TiO<sub>2</sub> nanotubes; AuPt alloy; photocatalysis; dye degradation; nanoparticles

## 1. Introduction

TiO<sub>2</sub> nanotubes (NTs) obtained by electrochemical anodization of a metallic Ti substrate are widely studied in photocatalytic applications due to their unique combination of geometry and functionality.[1] These nanotube arrays are directly grown vertically aligned from a metallic titanium substrate, with an easy control of the geometry during the synthesis via the electrochemical parameters. The large surface area, as well as their unique electronic and ionic properties,[1,2] make nanotubular structures suitable for many photoelectrochemical or photocatalytic applications, including pollutant degradation or water purification.[3–8]

In photocatalytic applications the TiO<sub>2</sub> photoexcited charge carriers react with the environment without an external applied voltage (in contrast to photoelectrochemical reactions). Under aerated conditions, conduction band electrons react with O<sub>2</sub> to form O<sub>2</sub>• radicals or superoxides, commonly referred to as reactive oxygen species (ROS) while valence band holes may be captured by water to form OH• radicals or may directly oxidize organic species to CO<sub>2</sub> and H<sub>2</sub>O. This effect is used for the photocatalytic degradation of unwanted pollutants in air or waste water. Overall, ROS species produced at the valence band and at the conduction band may contribute to efficient destruction of organic pollutants. In order to increase the efficiency by accelerating charge transfer reaction rates of the electron transfer to the environment, co-catalysts are frequently used.[8–12] Most commonly used co-catalysts on TiO<sub>2</sub> are noble metals (NM) such as Au, Pt or Pd,[13–16] which can lead to a beneficial Schottky junction and thus not only to a significantly improved charge transfer but also may provide catalytic features for the reactions of electrons with electron acceptors (mainly O<sub>2</sub>).[10,17] Other beneficial effects of some co-catalysts may be that visible light induced surface plasmon resonance effects can occur, enhancing the

1 light absorption region and therefore the catalytic activity in the visible light  
2 range.[8,18–20] The overall co-catalyst activity depends not only on the size and  
3  
4 distribution of the noble metal particles but also significantly on their relative  
5  
6 placement on the nanotubes.[8,21]  
7

8  
9 Usually, for NM@TiO<sub>2</sub> systems that are based on nanotubular structures, the  
10 deposition of metal particles is carried out by chemical or photoassisted chemical  
11 deposition[15,22,23] or by conventional sputtering.[23,24] Another common NM  
12 deposition approach is by sputtering-dewetting. Here first noble metal films are PVD-  
13 deposited on the top of highly organized TiO<sub>2</sub> nanotubes, and then these films are  
14 dewetted thermally, *i.e.* the film splits up into particles.[25–27] When sputtering  
15 noble metals on the tubular structures, the loading can be controlled, and the cluster  
16 size and distribution of the NM particles can be influenced by the dewetting  
17 conditions of the noble metal film – this allows to maximize the efficiency as co-  
18 catalyst for photocatalytic reactions.[25–28]  
19  
20  
21  
22  
23  
24  
25  
26  
27  
28  
29  
30  
31  
32

33  
34 Another most straightforward and unique approach to dope or decorate anodic  
35 TiO<sub>2</sub> nanotubular structures, is the growth of the nanotube layers from Ti-alloy  
36 substrates. For Ti-alloys with non-noble metals, such as Nb, Ru or Ta, during the  
37 anodic reaction these alloyed metals are oxidized and can lead to mixed-oxide or  
38 doped nanotubes – *i.e.*, these metal ions can be incorporated in the oxide lattice.[2] In  
39 contrast, for noble metals at low amounts *e.g.* < 1% for Au or Pt in the Ti alloy,[29–  
40 31] the NM is not oxidized but instead a self-decoration of the TiO<sub>2</sub> nanotubes with  
41 metallic nanoparticles (NP) takes place.[29,30]  
42  
43  
44  
45  
46  
47  
48  
49  
50  
51  
52

53 In the present work, we use both techniques: i) thin noble metal dewetted films,  
54 and ii) intrinsic noble decoration, and compare their effectiveness as photocatalyst.  
55  
56 For intrinsic decoration we use anodic oxidation of titanium alloys that contain either  
57  
58  
59  
60  
61  
62  
63  
64  
65

1 the individual noble metals such Au (Ti<sub>0.2</sub>at%Au), Pt (Ti<sub>0.2</sub>at%Pt), or both (i.e.  
2 Ti<sub>0.1</sub>at%Au<sub>0.1</sub>at%Pt), to produce uniformly and intrinsically NP decorated NTs, that  
3  
4 can then act as co-catalyst for the degradation of a model pollutant acid orange 7  
5 (AO7). For these tubes we find that the activity is significantly enhanced for the  
6  
7 intrinsic decoration with bimetallic AuPt compared with the single element tubes or  
8  
9 any extrinsically decorated NTs.  
10  
11  
12  
13

## 14 **2. Materials and Methods**

15  
16 For the nanotube preparation, Ti sheets (99.6 purity) of 0.2 mm thickness and  
17 alloys containing 0.2 at.% Au, 0.2 at.% Pt, 0.1 at.% Au + 0.1 at.% Pt were used  
18  
19 (purchased from HMW Hauner GmbH & Co). Prior to anodization, samples were  
20  
21 mechanically ground with #320, 800, 1200 and 2000 grit size SiC paper.  
22  
23 Subsequently, samples were degreased by sonication in acetone and ethanol, followed  
24  
25 by rinsing with deionized water and drying with nitrogen gas. Anodization was  
26  
27 performed in ethylene glycol containing 0.15 M NH<sub>4</sub>F at 45 V for 30 min in a two-  
28  
29 electrode system. After anodization, samples were immersed in ethanol for 20 min,  
30  
31 rinsed with deionized water, and dried with nitrogen. For the extrinsically decorated  
32  
33 samples, loading of the noble metal was done using plasma sputter deposition (Leica,  
34  
35 EM SCD500). All nanotubular samples (intrinsically and extrinsically decorated)  
36  
37 were annealed/dewetted at 450°C for 1 hour using a Rapid Thermal Annealer with a  
38  
39 heating and cooling rate of 30°C/min.  
40  
41  
42  
43  
44  
45  
46  
47

48 Morphological characterization was performed in a field-emission scanning  
49  
50 electron microscope (FE-SEM, Hitachi S-4800) and in a transmission electron  
51  
52 microscope (30 TEM/STEM Philips) coupled with EDS. The composition and  
53  
54 chemical state were characterized by X-ray photoelectron spectroscopy (XPS, PHI  
55  
56 5600, US), and peaks were shifted to C1s at 284.8 eV. For the crystallographic  
57  
58  
59  
60  
61  
62  
63  
64  
65

1 properties of the materials, X-ray diffraction (XRD, X'pert Philips MPD) equipped  
2 with a Panalytical X'celerator detector, with graphite monochromized Cu K $\alpha$  radiation  
3  
4 ( $\lambda = 1.54056 \text{ \AA}$ ) was used.  
5  
6

7 Elemental depth profile analysis was performed using a Horiba Jobin-Yvon 5000  
8 RF glow discharge optical emission spectroscopy (GDOES) instrument in an argon  
9 atmosphere of 650 Pa by applying an RF of 3000 MHz and a power of 27 W. Light  
10 emissions of characteristic wavelengths were monitored throughout the analysis with  
11 a sampling time of 0.1 s to obtain depth profiles. The signals were detected from a  
12 circular area of approximately 4 mm diameter.  
13  
14  
15  
16  
17  
18  
19  
20

21 The reflectance spectra of all the samples were measured by using a Lambda 950  
22 UV-VIS spectrometer with a 150 nm integrated sphere (Perkin Elmer) in the  
23 wavelength range of 800-200 nm (as background, a white-flat surface of BaSO $_4$  was  
24 employed).  
25  
26  
27  
28  
29  
30

31 For the photodegradation tests, the samples were immersed in a solution  $2.5 \times 10^{-5}$   
32 M of acid orange 7 (AO7) and were irradiated with a UV LED 365 nm ( $50 \text{ mW/cm}^2$ )  
33 for 2 h. Every 20 min the absorbance of the solution was measured in a UV/VIS  
34 Perkin Elmer Lambda XLS spectrophotometer.  
35  
36  
37  
38  
39  
40  
41  
42

### 43 **3. Results and discussion**

44 Figure 1a shows a schematic representation of the NTs used in this work: a) using  
45 intrinsic decoration by direct electrochemical anodization of the NM-alloy (NM: Au,  
46 Pt or both Au and Pt), and b) by using an extrinsic decoration of the tubes by  
47 sputtering, where particles are mainly present at the tube top. All nanotube layers  
48 were grown in a fluoride containing ethylene glycol electrolyte at 45 V for 30 min  
49 (more details are given in the experimental part) using the alloys or pure titanium as  
50  
51  
52  
53  
54  
55  
56  
57  
58  
59  
60  
61  
62  
63  
64  
65

1 substrates. Subsequently, the layers were converted to anatase by annealing in air at  
2 450 °C for 1 h. For the intrinsically decorated layers, metallic particles are observed  
3 not only at the top of the morphology (Figure 1b), but are also uniformly distributed  
4 along the NTs length, independently of the alloy used, as shown for NTs on TiAuPt in  
5 Figure 1d and for NTs on TiAu and TiPt alloys in Figures S1 and S2, respectively.  
6  
7  
8  
9

10  
11 All NT array layers exhibit similar thickness (i.e., a tube length of  $\approx 4 \mu\text{m}$ . Due to  
12 the low NM content in the alloys, the tube growth and morphology is not affected by  
13 the noble metal. For all intrinsic noble metals the uniform distribution of  
14 nanoparticles can be ascribed to a mechanism that has been reported for Au-Al  
15 alloys,[32] that is, the matrix metal is selectively oxidized out of the alloy leaving  
16 behind noble metal that accumulates to particles underneath at the metal/oxide  
17 interface. NM clusters then are decorated onto the growing oxide while the oxide tube  
18 grows.[33–35]  
19  
20  
21  
22  
23  
24  
25  
26  
27  
28  
29  
30

31 For extrinsically decorated TiO<sub>2</sub> nanotubes, Figure 1c shows an example of Au  
32 decorated TiO<sub>2</sub> NTs after sputtering, coating and dewetting; clearly, the Au layer is  
33 visible after dewetting as Au particles at the top of the nanotubes (see experimental  
34 part for details). Using this approach the Au nanoparticles have a maximum  
35 penetration depth of around 300 nm into the nanotubes (as observed in the cross-  
36 section SEM images, see also Figure S3).  
37  
38  
39  
40  
41  
42  
43  
44  
45

46 Figure 2a shows the XRD patterns of TiO<sub>2</sub> NTs before (*i*) and after annealing in air  
47 at 450°C for 1 hour (*ii*), after annealing only an anatase pattern is observed (besides  
48 the titanium peaks from the substrate). Before annealing, all as-formed nanotubes  
49 grown on either Ti or the noble metal alloys are amorphous. From the XRD patterns  
50 of TiO<sub>2</sub> nanotubes grown on alloys and annealed under similar conditions (i.e. (*iii*) -  
51 TiAu, and (*iv*) - TiPt alloy), not only anatase but also some traces of rutile can be  
52  
53  
54  
55  
56  
57  
58  
59  
60  
61  
62  
63  
64  
65

1 identified. However, no Au or Pt peaks are detected, due to the low concentration of  
2 the noble metals in both alloys (i.e. lower than the detection limit of XRD).  
3

4 From XPS, the Au4f and Pt4f peaks can easily be evaluated in the intrinsically  
5 decorated NTs, namely NTs grown on the TiAu, TiPt and TiAuPt alloys (Figure 2b  
6 and c, using as reference a TiO<sub>2</sub> NTs layer grown on Ti), as well as for the  
7 extrinsically doped tubes (Figure S4). The composition evaluated from the XPS data  
8 of the intrinsically decorated nanotubes, i.e. grown on Ti0.2at%Au, Ti0.2at%Pt alloys  
9 or on TiAuPt (0.1at%Au and 0.1at%Pt) – see Table S1, is in good correlation with  
10 their nominal noble metal amount. Considering the Au and Pt peak positions for the  
11 intrinsic and extrinsic decorations, it is worth mentioning that the Au + Pt extrinsic  
12 decoration (sputtered 1 nm Au and 1 nm Pt, followed by dewetting) on the NTs shows  
13 no shift in the Au4f and Pt4f peak positions, namely the Au4f<sub>7/2</sub> is at ≈83.53 eV and  
14 the Pt4f<sub>7/2</sub> is ≈70.61 eV (as shown in Figure S4).  
15  
16  
17  
18  
19  
20  
21  
22  
23  
24  
25  
26  
27  
28  
29  
30

31 In contrast, for intrinsically decorated NTs, we observe a shift in the Au4f peak  
32 and Pt4f peak that together with TEM-EDS investigations confirm the alloy nature of  
33 the nanoparticles (Figure 2d-f and Table S2).[31,36]  
34  
35  
36  
37  
38

39 In order to characterize the distribution of the NM nanoparticles we carried out  
40 XPS and GDOES measurements of such layers. The XPS sputter depth profile of the  
41 first 300 nm of the intrinsically decorated nanotubes with AuPt particles (Figure S8a),  
42 i.e. nanotubes grown on the TiAuPt alloy, confirms that similar amounts of Au and Pt  
43 of ≈0.1 at% are present. To obtain the distribution over the entire length, glow  
44 discharge optical emission spectroscopy (GDOES) sputter depth profiles were  
45 acquired resulting in similar amounts of Au and Pt content throughout the length of  
46 the NTs on TiAuPt alloy (using as reference NTs on pure Ti) – as shown in Figure  
47 S8b, for more details see supporting information. To compare the overall loading of  
48  
49  
50  
51  
52  
53  
54  
55  
56  
57  
58  
59  
60  
61  
62  
63  
64  
65

1 the tubes with noble metals, namely to compare the PVD coated and intrinsic layers,  
2 we performed EDX analysis as given in Table S3. The data shows that in all cases a  
3 composition close to the nominal values was obtained – but more importantly that the  
4 overall amount of noble metal after PVD is comparable to the intrinsic amount.  
5  
6  
7

8  
9 These tubes were then used to investigate the photocatalytic degradation of the  
10 model pollutant (AO7). Figure 3a shows the kinetics of the photodegradation of AO7  
11 for intrinsically decorated TiO<sub>2</sub> NTs and Figure 3b shows the kinetics for extrinsically  
12 decorated NTs. From these data, the kinetic constants can be evaluated (compiled in  
13 Figure 3c). Overall, for Au decoration a beneficial effect on the degradation  
14 efficiency of AO7 can be observed. However, it is also evident that a decrease in  
15 photoefficiency is observed when only Pt is present, both for intrinsic and extrinsic  
16 decoration of the tubes. This can be ascribed to an inactivation of the co-catalyst by  
17 forming Pt oxides as a result of annealing in air, as indicated by the XPS data in  
18 Figure S4-S7.[24,37] Clearly, a signature of PtO is obtained for these tubes (Figure  
19 S4 and S6). If one compares nanotubes with extrinsic decoration and with intrinsic  
20 decoration, clearly much higher efficiencies are obtained for the intrinsic decoration.  
21 This may be ascribed to the combination of particle size and distribution as well as  
22 their embedding in the nanotube wall. However, most remarkable is that the  
23 synergetic effect in the photodegradation of AO7 observed for the alloyed  
24 nanoparticles intrinsically decorated on the NTs (NTs grown on TiAuPt alloy) is not  
25 present for the Au+Pt nanoparticles decorated extrinsically onto the NTs, i.e. if this  
26 enhancement would only be related to the simultaneous presence of both noble metals  
27 (Au and Pt), then it follows that the Au+Pt nanoparticles decorated onto tubes would  
28 also have a higher efficiency than the elements alone. However, as this is not the case  
29 we ascribe the enhanced photocatalytic activity for AO7 of the intrinsically decorated  
30  
31  
32  
33  
34  
35  
36  
37  
38  
39  
40  
41  
42  
43  
44  
45  
46  
47  
48  
49  
50  
51  
52  
53  
54  
55  
56  
57  
58  
59  
60  
61  
62  
63  
64  
65

1 tubes to the formation of mixed AuPt alloy nanoparticles that takes place only for the  
2 intrinsic decoration (i.e. obtained as a result of anodizing TiAuPt alloys).  
3

4  
5 In order to explore if additional plasmonic effects contribute to the photocatalytic  
6 efficiency, we performed reflectivity measurements for the tubes that were decorated  
7 with nanoparticles (Figure S9). For the nanotubes decorated intrinsically with Pt or  
8 AuPt, no plasmon resonance was observed. However, in presence of Au nanoparticles  
9 extrinsically decorated onto the nanotubes, a plasmonic effect is apparent (i.e., a clear  
10 plasmonic band is only visible for 2 nm nominal thickness Au decoration or partially  
11 for nanotubes grown on the TiAu alloy with 0.2at% Au). From these data it can be  
12 concluded that the enhancement in the photodegradation reactions of the intrinsically  
13 decorated nanotubes with the mixed AuPt nanoparticles is not due to plasmonic  
14 features.  
15  
16  
17  
18  
19  
20  
21  
22  
23  
24  
25  
26  
27  
28

29 Previous works on electrocatalysis have reported an enhanced rate for the oxygen  
30 reduction reaction (ORR) on AuPt compared with the same loading of Pt or Au alone.  
31 A key effect was attributed to the ability of Au atoms to provide Au-OH<sub>ads</sub>  
32 intermediates that are formed from O<sub>2</sub> and water that then can easily react with  
33 neighboring Pt atoms to form a range of ROS-products. In other words, on an AuPt  
34 alloy the electron transfer to the electrolyte oxygen becomes accelerated which also  
35 diminishes electron recombination with valence band holes – thus enabling a higher  
36 life-time of holes and therefore a higher reaction possibility of the holes with the  
37 organic compound to oxidatively destroy it. As a result, bimetallic AuPt co-catalysts  
38 on titania NTs show a much higher photocatalytic activity for AO7 degradation  
39 compared to a plain combination of Au or Pt nanoparticles. This is evident by the  
40 comparison with Au and Pt nanoparticles that were fabricated on the NTs by  
41 sputtering and dewetting. In this case no bimetallic alloyed particles are formed and  
42  
43  
44  
45  
46  
47  
48  
49  
50  
51  
52  
53  
54  
55  
56  
57  
58  
59  
60  
61  
62  
63  
64  
65

1 the photocatalytic dye degradation tests do not show a synergetic effect of Au and Pt  
2 features.  
3

#### 4 **4. Conclusions**

5  
6  
7 In conclusion, we demonstrate that bimetallic AuPt decorated TiO<sub>2</sub> nanotubes can  
8 efficiently be produced by anodization of Ti-Au-Pt alloys, while only individual Au +  
9 Pt nanoparticle decoration is achieved by an element sputtering/dewetting approach.  
10 We show that the intrinsically formed bimetallic AuPt co-catalytic particles show a  
11 synergetic beneficial co-catalytic effect in the photocatalytic destruction of pollutants  
12 when using TiO<sub>2</sub> nanotubes. This synergy is absent if Au and Pt are present as  
13 individual decorations on the tubes. We ascribe the overall effect to a facilitated ORR  
14 on the bimetallic AuPt co-catalyst; this leads to an enhanced ROS production at the  
15 conduction band and at the valence band which in turn provide an enhanced pollutant  
16 degradation rate.  
17  
18  
19  
20  
21  
22  
23  
24  
25  
26  
27  
28  
29  
30

#### 31 **Acknowledgements**

32  
33 We would like to acknowledge the ERC, the DFG, the Erlangen DFG cluster of  
34 excellence EAM, project EXC 315 (Bridge), the DFG funCOS for financial support.  
35  
36 Shiva Mohajernia is acknowledged for XPS measurements.  
37  
38  
39  
40  
41  
42  
43

#### 44 **Supporting Information**

45 Supporting Information is available in the attached file.  
46  
47

#### 48 **Conflicts of interest**

49 There are no conflicts to declare.  
50  
51  
52  
53  
54  
55  
56  
57  
58  
59  
60  
61  
62  
63  
64  
65

## References

- 1  
2  
3  
4  
5  
6  
7  
8  
9  
10  
11  
12  
13  
14  
15  
16  
17  
18  
19  
20  
21  
22  
23  
24  
25  
26  
27  
28  
29  
30  
31  
32  
33  
34  
35  
36  
37  
38  
39  
40  
41  
42  
43  
44  
45  
46  
47  
48  
49  
50  
51  
52  
53  
54  
55  
56  
57  
58  
59  
60  
61  
62  
63  
64  
65
- [1] P. Roy, S. Berger, P. Schmuki, TiO<sub>2</sub> nanotubes: synthesis and applications, *Angew. Chem. Int. Ed.* 50 (2011) 2904–2939. doi:10.1002/anie.201001374.
  - [2] K. Lee, A. Mazare, P. Schmuki, One-dimensional titanium dioxide nanomaterials: nanotubes, *Chem. Rev.* 114 (2014) 9385–9454. doi:10.1021/cr500061m.
  - [3] P. Roy, D. Kim, K. Lee, E. Spiecker, P. Schmuki, TiO<sub>2</sub> nanotubes and their application in dye-sensitized solar cells., *Nanoscale.* 2 (2010) 45–59. doi:10.1039/b9nr00131j.
  - [4] J. Gong, J. Liang, K. Sumathy, Review on dye-sensitized solar cells (DSSCs): Fundamental concepts and novel materials, *Renew. Sustain. Energy Rev.* 16 (2012) 5848–5860. doi:10.1016/J.RSER.2012.04.044.
  - [5] S. Park, S. Kim, S. Park, W. Lee, C. Lee, Effects of Functionalization of TiO<sub>2</sub> Nanotube Array Sensors with Pd Nanoparticles on Their Selectivity, *Sensors.* 14 (2014) 15849–15860. doi:10.3390/s140915849.
  - [6] K. Siuzdak, R. Bogdanowicz, M. Sawczak, M. Sobaszek, Enhanced capacitance of composite TiO<sub>2</sub> nanotube/boron-doped diamond electrodes studied by impedance spectroscopy, *Nanoscale.* 7 (2015) 551–558. doi:10.1039/C4NR04417G.
  - [7] Q. Gui, Z. Xu, H. Zhang, C. Cheng, X. Zhu, M. Yin, Y. Song, L. Lu, X. Chen, D. Li, Enhanced Photoelectrochemical Water Splitting Performance of Anodic TiO<sub>2</sub> Nanotube Arrays by Surface Passivation, *ACS Appl. Mater. Interfaces.* 6 (2014) 17053–17058. doi:10.1021/am504662w.
  - [8] I. Paramasivam, H. Jha, N. Liu, P. Schmuki, A review of photocatalysis using self-organized TiO<sub>2</sub> nanotubes and other ordered oxide nanostructures., *Small.* 8 (2012) 3073–3103. doi:10.1002/smll.201200564.
  - [9] A. Fujishima, T.N. Rao, D.A. Tryk, Titanium dioxide photocatalysis, *J. Photochem. Photobiol. C Photochem. Rev.* 1 (2000) 1–21. doi:10.1016/S1389-5567(00)00002-2.
  - [10] A. Fujishima, X. Zhang, D. Tryk, TiO<sub>2</sub> photocatalysis and related surface phenomena, *Surf. Sci. Rep.* 63 (2008) 515–582. doi:10.1016/j.surfrep.2008.10.001.
  - [11] A.I. Kontos, V. Likodimos, T. Stergiopoulos, D.S. Tsoukleris, P. Falaras, I.

- 1 Rabias, G. Papavassiliou, D. Kim, J. Kunze, P. Schmuki, Self-Organized  
2 Anodic TiO<sub>2</sub> Nanotube Arrays Functionalized by Iron Oxide Nanoparticles,  
3 Chem. Mater. 21 (2009) 662–672. doi:10.1021/cm802495p.  
4
- 5 [12] H.Y. Yang, S.F. Yu, S.P. Lau, X. Zhang, D.D. Sun, G. Jun, Direct growth of  
6 ZnO nanocrystals onto the surface of porous TiO<sub>2</sub> nanotube arrays for highly  
7 efficient and recyclable photocatalysts., Small. 5 (2009) 2260–2264.  
8 doi:10.1002/smll.200900724.  
9
- 10 [13] X. Chen, S.S. Mao, Titanium dioxide nanomaterials: synthesis, properties,  
11 modifications, and applications., Chem. Rev. 107 (2007) 2891–2959.  
12 doi:10.1021/cr0500535.  
13
- 14 [14] S.K. Mohapatra, N. Kondamudi, S. Banerjee, M. Misra, Functionalization of  
15 Self-Organized TiO<sub>2</sub> Nanotubes with Pd Nanoparticles for Photocatalytic  
16 Decomposition of Dyes under Solar Light Illumination, Langmuir. 24 (2008)  
17 11276–11281. doi:10.1021/la801253f.  
18
- 19 [15] I. Paramasivam, J.M. Macak, P. Schmuki, Photocatalytic activity of TiO<sub>2</sub>  
20 nanotube layers loaded with Ag and Au nanoparticles, Electrochem. Commun.  
21 10 (2008) 71–75. doi:10.1016/J.ELECOM.2007.11.001.  
22
- 23 [16] H. Yu, X. Wang, H. Sun, M. Huo, Photocatalytic degradation of malathion in  
24 aqueous solution using an Au–Pd–TiO<sub>2</sub> nanotube film, J. Hazard. Mater. 184  
25 (2010) 753–758. doi:10.1016/J.JHAZMAT.2010.08.103.  
26
- 27 [17] M.A. Nadeem, M. Murdoch, G.I.N. Waterhouse, J.B. Metson, M.A. Keane, J.  
28 Llorca, H. Idriss, Photoreaction of ethanol on Au/TiO<sub>2</sub> anatase: Comparing the  
29 micro to nanoparticle size activities of the support for hydrogen production, J.  
30 Photochem. Photobiol. A Chem. 216 (2010) 250–255.  
31 doi:10.1016/J.JPHOTOCHEM.2010.07.007.  
32
- 33 [18] S.K. Ghosh, T. Pal, Interparticle Coupling Effect on the Surface Plasmon  
34 Resonance of Gold Nanoparticles: From Theory to Applications, Chem. Rev.  
35 107 (2007) 4797–4862. doi:10.1021/CR0680282.  
36
- 37 [19] H. Zhang, G. Chen, D.W. Bahnemann, Photoelectrocatalytic materials for  
38 environmental applications, J. Mater. Chem. 19 (2009) 5089–5121.  
39 doi:10.1039/b821991e.  
40
- 41 [20] A. Naldoni, F. Riboni, U. Guller, A. Boltasseva, V.M. Shalaev, A. V.  
42 Kildishev, Solar-Powered Plasmon-Enhanced Heterogeneous Catalysis,  
43 Nanophotonics. 5 (2016) 112.  
44  
45  
46  
47  
48  
49  
50  
51  
52  
53  
54  
55  
56  
57  
58  
59  
60  
61  
62  
63  
64  
65

- 1  
2  
3  
4  
5  
6  
7  
8  
9  
10  
11  
12  
13  
14  
15  
16  
17  
18  
19  
20  
21  
22  
23  
24  
25  
26  
27  
28  
29  
30  
31  
32  
33  
34  
35  
36  
37  
38  
39  
40  
41  
42  
43  
44  
45  
46  
47  
48  
49  
50  
51  
52  
53  
54  
55  
56  
57  
58  
59  
60  
61  
62  
63  
64  
65
- [21] X. Zhou, N. Liu, P. Schmuki, Photocatalysis with TiO<sub>2</sub> Nanotubes: “Colorful” Reactivity and Designing Site-Specific Photocatalytic Centers into TiO<sub>2</sub> Nanotubes, *ACS Catal.* 7 (2017) 3210–3235. doi:10.1021/acscatal.6b03709.
- [22] J. Kiwi, M. Graetzel, Optimization of conditions for photochemical water cleavage. Aqueous platinum/TiO<sub>2</sub> (anatase) dispersions under ultraviolet light, *J. Phys. Chem.* 88 (1984) 1302–1307. doi:10.1021/j150651a012.
- [23] Y.-Y. Song, Z.-D. Gao, P. Schmuki, Highly uniform Pt nanoparticle decoration on TiO<sub>2</sub> nanotube arrays: A refreshable platform for methanol electrooxidation, *Electrochem. Commun.* 13 (2011) 290–293. doi:10.1016/j.elecom.2011.01.006.
- [24] J. Yoo, M. Altomare, M. Mokhtar, A. Alshehri, S.A. Al-Thabaiti, A. Mazare, P. Schmuki, Photocatalytic H<sub>2</sub> Generation Using Dewetted Pt-Decorated TiO<sub>2</sub> Nanotubes: Optimized Dewetting and Oxide Crystallization by a Multiple Annealing Process, *J. Phys. Chem. C.* 120 (2016) 15884–15892. doi:10.1021/acs.jpcc.5b12050.
- [25] J.E. Yoo, K. Lee, M. Altomare, E. Selli, P. Schmuki, Self-organized arrays of single-metal catalyst particles in TiO<sub>2</sub> cavities: a highly efficient photocatalytic system., *Angew. Chem. Int. Ed.* 52 (2013) 7514–7517. doi:10.1002/anie.201302525.
- [26] J. Yoo, K. Lee, P. Schmuki, Dewetted Au films form a highly active photocatalytic system on TiO<sub>2</sub> nanotube-stumps, *Electrochem. Commun.* 34 (2013) 351–355. doi:10.1016/j.elecom.2013.07.008.
- [27] N.T. Nguyen, J. Yoo, M. Altomare, P. Schmuki, “Suspended” Pt nanoparticles over TiO<sub>2</sub> nanotubes for enhanced photocatalytic H<sub>2</sub> evolution., *Chem. Commun.* 50 (2014) 9653–9656. doi:10.1039/c4cc04087b.
- [28] M. Altomare, N.T. Nguyen, P. Schmuki, Templated Dewetting: Designing Entirely Self-Organized Platforms for Photocatalysis, *Chem. Sci.* 7 (2016) 6865–6886. doi:10.1039/C6SC02555B.
- [29] K. Lee, R. Hahn, M. Altomare, E. Selli, P. Schmuki, Intrinsic Au decoration of growing TiO<sub>2</sub> nanotubes and formation of a high-efficiency photocatalyst for H<sub>2</sub> production., *Adv. Mater.* 25 (2013) 6133–6137. doi:10.1002/adma.201302581.
- [30] S.N. Basahel, K. Lee, R. Hahn, P. Schmuki, S.M. Bawaked, S. a Al-Thabaiti, Self-decoration of Pt metal particles on TiO<sub>2</sub> nanotubes used for highly efficient photocatalytic H<sub>2</sub> production., *Chem. Commun.* 50 (2014) 6123–

6125. doi:10.1039/c4cc01287a.

- 1  
2  
3  
4  
5  
6  
7  
8  
9  
10  
11  
12  
13  
14  
15  
16  
17  
18  
19  
20  
21  
22  
23  
24  
25  
26  
27  
28  
29  
30  
31  
32  
33  
34  
35  
36  
37  
38  
39  
40  
41  
42  
43  
44  
45  
46  
47  
48  
49  
50  
51  
52  
53  
54  
55  
56  
57  
58  
59  
60  
61  
62  
63  
64  
65
- [31] H. Bian, N.T. Nguyen, J. Yoo, S. Hejazi, S. Mohajernia, J. Müller, E. Spiecker, H. Tsuchiya, O. Tomanec, B.E. Sanabria-Arenas, R. Zboril, Y.Y. Li, P. Schmuki, Forming a Highly Active, Homogeneously Alloyed AuPt Co-catalyst Decoration on TiO<sub>2</sub> Nanotubes Directly During Anodic Growth, *ACS Appl. Mater. Interfaces*. 10 (2018) 18220–18226. doi:10.1021/acsami.8b03713.
- [32] S.J. Garcia-Vergara, M. Curioni, F. Roeth, T. Hashimoto, P. Skeldon, G.E. Thompson, H. Habazaki, Incorporation of Gold into Porous Anodic Alumina Formed on an Al–Au Alloy, *J. Electrochem. Soc.* 155 (2008) C333–C339. doi:10.1149/1.2917214.
- [33] O. Jessensky, F. Müller, U. Gösele, Self-Organized Formation of Hexagonal Pore Structures in Anodic Alumina, *J. Electrochem. Soc.* 145 (1998) 3735–3740. doi:10.1149/1.1838867.
- [34] W. Lee, K. Schwirn, M. Steinhart, E. Pippel, R. Scholz, U. Gösele, Structural engineering of nanoporous anodic aluminium oxide by pulse anodization of aluminium, *Nat. Nanotechnol.* 3 (2008) 234–239. doi:10.1038/nnano.2008.54.
- [35] J.E. Houser, K.R. Hebert, Modeling the Potential Distribution in Porous Anodic Alumina Films during Steady-State Growth, *J. Electrochem. Soc.* 153 (2006) B566–B573. doi:10.1149/1.2360763.
- [36] D. Tongsakul, S. Nishimura, K. Ebitani, Platinum/gold alloy nanoparticles-supported hydrotalcite catalyst for selective aerobic oxidation of polyols in base-free aqueous solution at room temperature, *ACS Catal.* 3 (2013) 2199–2207. doi:10.1021/cs400458k.
- [37] J. Lee, W. Choi, Photocatalytic Reactivity of Surface Platinized TiO<sub>2</sub>: Substrate Specificity and the Effect of Pt Oxidation State, *J. Phys. Chem. B.* 109 (2005) 7399–7406. doi:10.1021/JP044425+.

1  
2  
3  
4  
5  
6  
7  
8  
9  
10  
11  
12  
13  
14  
15  
16  
17  
18  
19  
20  
21  
22  
23  
24  
25  
26  
27  
28  
29  
30  
31  
32  
33  
34  
35  
36  
37  
38  
39  
40  
41  
42  
43  
44  
45  
46  
47  
48  
49  
50  
51  
52  
53  
54  
55  
56  
57  
58  
59  
60  
61  
62  
63  
64  
65

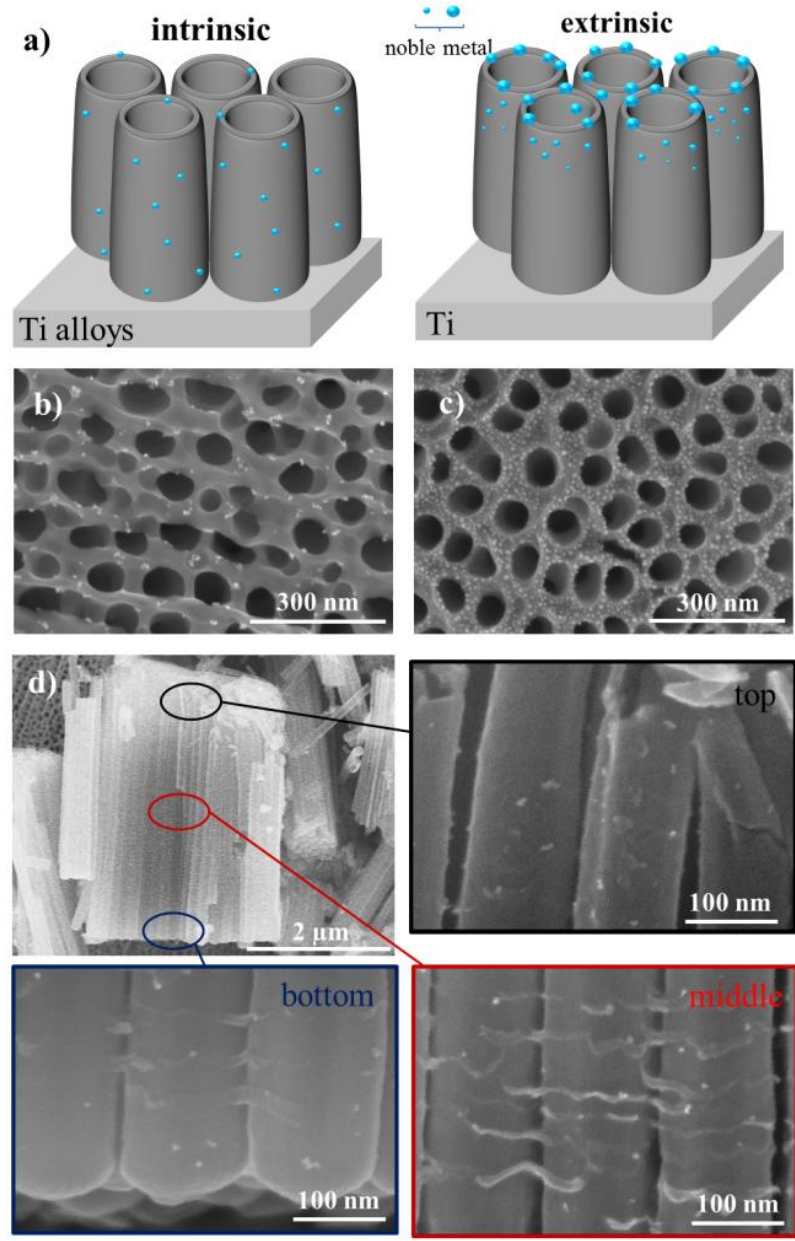


**Figure 1.** a) Schematic representation of  $\text{TiO}_2$  NTs intrinsically decorated by direct anodization of alloy (left) and extrinsically decorated by sputtering and dewetting a noble metal on the top of the NTs anodically growth on Ti foil (right); b) Top view of the NTs on TiAuPt alloy; c) Top view of the Ti NTs with 1 nm of Au dewetted and d) Cross section of the NTs on TiAuPt alloy with magnifications in the top, middle and bottom part.

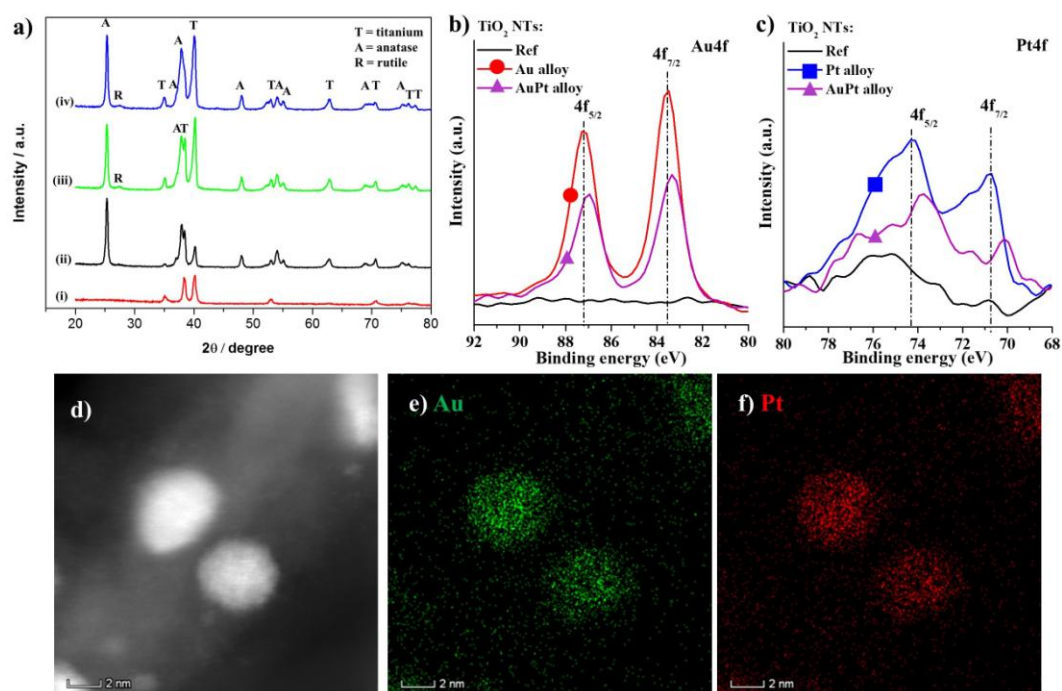


**Figure 2.** a) XRD patterns of (i) as-formed TiO<sub>2</sub> NTs; (ii) annealed at 450°C TiO<sub>2</sub> NTs; (iii) NTs on TiAu and (iv) NTs on TiPt alloys. b) and c) high resolution XPS spectra of Au4f and Pt4f for NTs on Ti (Ref) and on TiPt (Pt alloy), TiAu (Au alloy) and TiAuPt (AuPt alloy) alloys. d) TEM image of AuPt nanoparticle on the top of NTs grown on TiAuPt alloy. TEM-EDS elemental mapping of e) Au and f) Pt in the selected region of d).

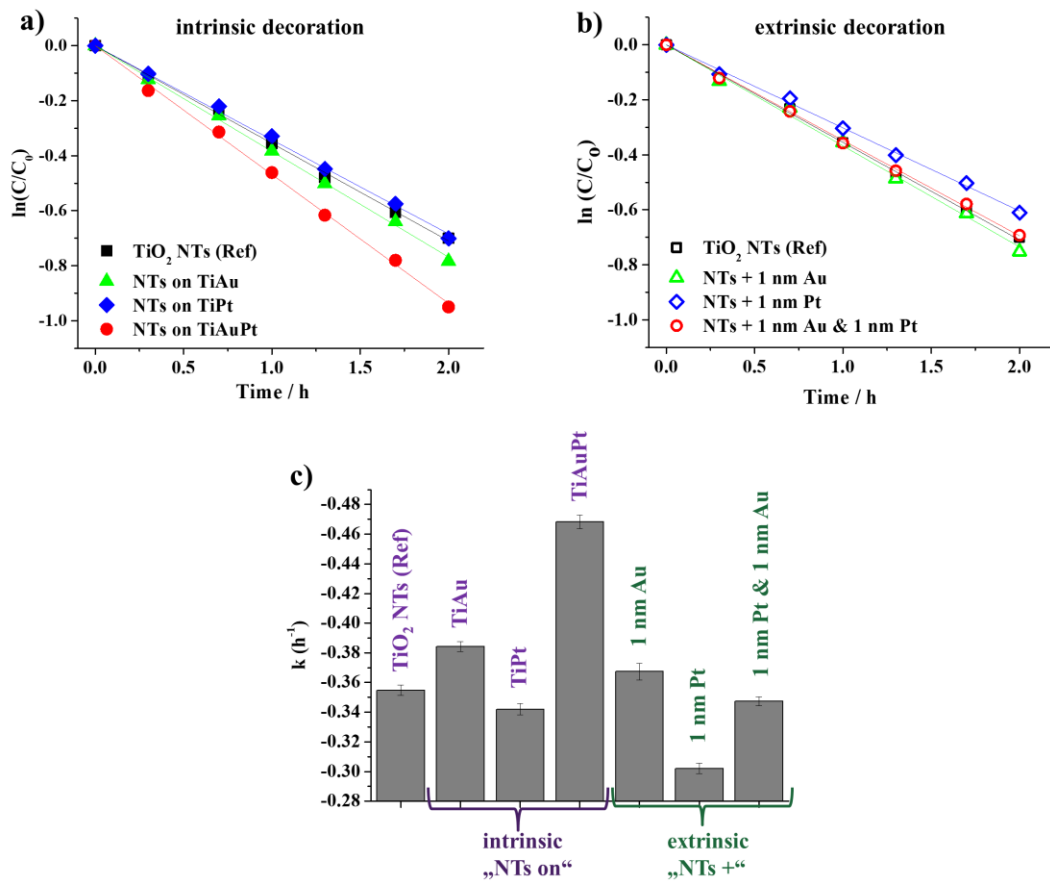
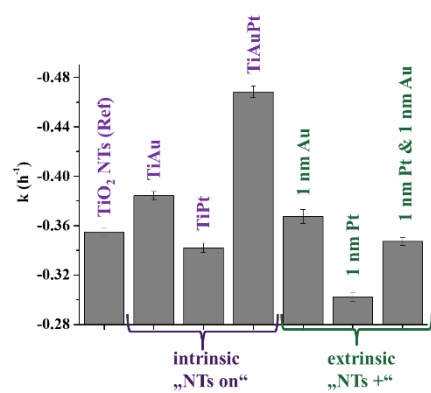


**Figure 3.** Photodegradation curves of AO7 with: a) intrinsically and b) extrinsically decorated TiO<sub>2</sub> NTs; (c) kinetic constants of AO7 degradation with intrinsically and extrinsically decorated TiO<sub>2</sub> NTs.

### Graphic abstract



### Highlights

- AuPt alloy particles can intrinsically be decorated on anodicTiO<sub>2</sub> nanotubes
- Anodization is carried out using AuPtTi alloys
- Alternatively extrinsic noble metal decoration is done by sputter-dewetting
- The photocatalytic activity for intrinsically decorated tubes is significantly higher than for extrinsic decoration